Priming with real motion biases visual cortical response to bistable apparent motion

Qing-fang Zhang[a,1], Yunqing Wen[a,1], Deng Zhang[a], Liang She[a], Jian-young Wu[b], Yang Dan[c,d], and Mu-ming Poo[a,c,2]

[a]Institute of Neuroscience, State Key Laboratory of Neuroscience, Shanghai Institutes for Biological Sciences, Chinese Academy of Sciences, Shanghai 200031, China; [b]Department of Neuroscience, Georgetown University Medical Center, Washington, DC 20057-1460; and [c]Department of Molecular and Cell Biology and [d]Howard Hughes Medical Institute, University of California, Berkeley, CA 94720

Contributed by Mu-ming Poo, October 28, 2012 (sent for review September 17, 2012)

Apparent motion quartet is an ambiguous stimulus that elicits bistable perception, with the perceived motion alternating between two orthogonal paths. In human psychophysical experiments, the probability of perceiving motion in each path is greatly enhanced by a brief exposure to real motion along that path. To examine the neural mechanism underlying this priming effect, we used voltage-sensitive dye (VSD) imaging to measure the spatiotemporal activity in the primary visual cortex (V1) of awake mice. We found that a brief real motion stimulus transiently biased the cortical response to subsequent apparent motion toward the spatiotemporal pattern representing the real motion. Furthermore, intracellular recording from V1 neurons in anesthetized mice showed a similar increase in subthreshold depolarization in the neurons representing the path of real motion. Such short-term plasticity in early visual circuits may contribute to the priming effect in bistable visual perception.

In bistable perception, an ambiguous sensory stimulus gives rise to two mutually exclusive interpretations, and switches between the two percepts can occur spontaneously without any change in the visual input. Such dissociation between the sensory input and perceptual interpretation provides a unique opportunity for studying the neural correlates of conscious awareness (1, 2). A well-known example of bistable perception is that induced by apparent motion quartet, consisting of a pair of dots flashed alternately at the two diagonals of an invisible square (3). The pair of dots is perceived to move back and forth, along either the vertical or horizontal edges of the square, and the switch between these two percepts occurs spontaneously. Similar bistable perception was demonstrated in the somatosensory system using vibrotactile stimuli presented to the finger pad (4), suggesting that bistable perception of ambiguous motion is mediated by a general mechanism shared across sensory modalities.

An important step in elucidating the neural mechanism underlying bistable perception is to identify the brain regions in which the neuronal activity reflects the changing perception under constant sensory stimuli. Visual psychophysical studies have shown that the perception of apparent motion along a given path impaired identification of a visual target in the path, suggesting that the illusory motion is represented explicitly by some visual neurons (5). A functional MRI (fMRI) study in human subjects has revealed apparent motion-related activity in the primary visual cortex (V1) regions retinotopically mapped to the motion path (6). During the apparent motion quartet stimulus, the fMRI signal was correlated with the perceptual switches, suggesting a neural correlate of bistable perception in V1. However, the relationship between neuronal activity and the blood-oxygen-level–dependent (BOLD) signal measured with fMRI is indirect and complex (7, 8). To understand the role of V1 in bistable perception, it is important to make direct measurements of V1 electrical activity in response to the ambiguous stimuli.

In this study, we examined the contribution of V1 to the perception of apparent motion by measuring a priming effect induced by real motion. In human psychophysical experiments, we showed that a brief exposure to real motion stimulus strongly enhanced the perception of apparent motion along the same path. In voltage-sensitive dye (VSD) imaging experiments in awake mice, such a real motion stimulus caused a transient increase in the cortical activity representing the motion path during subsequent cycles of apparent motion. In vivo whole-cell recordings in anesthetized mice further revealed real motion-induced potentiation of synaptic inputs to the neurons whose receptive fields fell along the motion path. Together, these results suggest that short-term plasticity in the primary visual cortex may participate in the priming effect in bistable perception of ambiguous motion stimuli.

Results

We used VSD imaging to measure the spatiotemporal pattern of activity in V1 of awake mice that were head restrained on a spherical treadmill (Fig. 1*A* and *Materials and Methods*). To determine the retinotopic representation of the dot quartet for each mouse, we first measured the cortical response to each of the four dots. Recordings were performed when the running speed of the mouse was <20 mm/s and the eye movement was very small (*Materials and Methods*, *SI Materials and Methods*, and Fig. S1). The bright dot (7° in diameter) was flashed briefly (100 ms) at each of the four corners of a diamond (positions 1–4, Fig. 1*A*). The cortical location of the response to each dot was determined by averaging the responses from five trials (Fig. 1*B*, white and black squares mark the maximal responses). The dots were arranged in a diamond with oblique sides rather than in a square, because the distance between corresponding cortical areas for two dots of equal distance was larger along the vertical direction than along the horizontal direction.

In human psychophysical experiments using similar quartet stimuli, we found a potent priming effect of a real motion to the apparent motion. The subjects mostly reported an apparent motion along path A or path B, if a single cycle of real motion (consisting of a forward and a backward sweep) along path A or B was presented before the apparent motion stimuli, respectively (Fig. S2). To examine the neural mechanism of this positive priming effect in awake mice, we measured the impact of a brief real motion stimulus (sweeping dots) on V1 responses to subsequent apparent motion stimuli (flashing dots). In each trial, the visual stimulus started with four cycles of apparent motion quartet, followed by one cycle of real motion along either path A ($1 \leftrightarrow 2$, $3 \leftrightarrow 4$) or path B ($1 \leftrightarrow 3$, $2 \leftrightarrow 4$), and six additional cycles of apparent motion (Fig. 2 *A* and *B*, *Upper*). We found that each real motion stimulus evoked strong responses in the cortical regions corresponding to the motion path (Fig. 2 *A* and *B*), between the locations of maximal responses to the flashed dots (black and white squares). To clearly distinguish the responses to real motion along path A and path B, we computed their difference (Fig. 2*C*), which shows positive activity ($A > B$) at the cortical locations representing path A (red arrowheads) and negative activity ($A < B$)

Author contributions: Q.-f.Z., Y.W., Y.D., and M.-m.P. designed research; Q.-f.Z., Y.W., and D.Z. performed research; J.-y.W. contributed new reagents/analytic tools; Q.-f.Z., Y.W., D.Z., and L.S. analyzed data; and Q.-f.Z., Y.W., J.-y.W., Y.D., and M.-m.P. wrote the paper.

The authors declare no conflict of interest.

[1] Q.-f.Z. and Y.W. contributed equally to this work.

[2] To whom correspondence should be addressed. E-mail: mpoo@berkeley.edu.

This article contains supporting information online at www.pnas.org/lookup/suppl/doi:10.1073/pnas.1218654109/-/DCSupplemental.

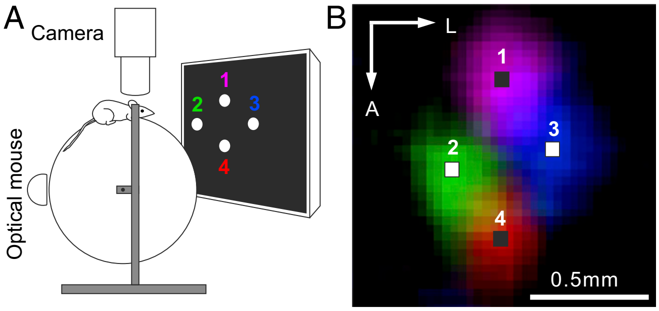

Fig. 1. Methods of VSD imaging from awake head-fixed mice. (*A*) Schematic diagram of the head-fixed setup. (*B*) VSD signals in response to each of four bright dots (7° in diameter) flashed separately on the video screen, during 50–90 ms after the onset of the flash. Signals were color coded for the four dots shown in *A*. Black and white squares represent the region of maximal VSD signals evoked by the four flash dots.

at those for path B (blue arrowheads, Fig. 2*C*). To combine the results from all of the experiments, the spatial pattern of cortical response measured in each mouse was transformed (through rotation and stretching) into an idealized cortical map in which the maximal responses to the four dots fell on a perfect diamond (*Materials and Methods*). The average differential response (path A – path B, hereafter referred to as "Δ response") across experiments also showed clear positive and negative responses in regions representing paths A and B, respectively (Fig. 2*D*).

We then asked whether the single cycle of the real motion affected the cortical responses to subsequent cycles of apparent motion stimuli. We computed the difference in the response to apparent motion between those immediately following the real motion in path A (Fig. 3*A*) and path B (Fig. 3*B*). We found that, although the visual stimuli during the apparent motion period were identical between the two types of trials, there was a clear difference in the cortical response immediately after the real motion (Fig. 3*C*). The Δ response was positive at the cortical regions representing path A (red arrowheads) and negative at those representing path B (blue arrowheads), similar to the Δ response to the real motion (Fig. 2*C*). A similar pattern was also found in the population average of Δ response (Fig. 3*D*, $n = 19$ mice). The similarity to the Δ response for the real motion was most striking during the first set of apparent motion stimuli immediately following the real motion and became weaker but still discernible for the second set of apparent motion stimuli. By contrast, the Δ response for the apparent motion period before the real motion period showed no consistent activity in the cortical regions that showed induced activities after the real motion stimuli (Fig. S3).

To quantify the effect of the real motion on cortical responses to apparent motion, we measured the amplitude of the Δ response as a function of time (Fig. 4*A*) in the cortical regions representing path A (red trace) and path B (blue trace) and computed their difference (Fig. 4*B*). We found that the activity difference showed two large peaks, corresponding to the forward and backward sweeps of the real motion. Interestingly, during subsequent cycles of the apparent motion, the difference trace showed several cycles of oscillation at the temporal frequency of the real and apparent motion (Fig, 4*B*, arrows), although the amplitude was progressively smaller. Such oscillation was absent during the apparent motion stimuli before the real motion, indicating that it is induced by the real motion stimuli. To further quantify the effect, we used the spatial temporal pattern of the Δ response to a single sweep of the real motion as a template and measured its similarity to the Δ response for apparent motion stimuli by the correlation coefficient (CC). We found that the Δ response for the apparent motion showed significant similarity to that for the real motion in the first set of the apparent motion following the real motion (Fig. 4 *C* and *D*, $P = 3 \times 10^{-8}$, unpaired *t* test). Thus, a brief exposure to a real motion caused a transient increase of the cortical representation of the motion path during subsequent apparent motion stimuli.

We note that the signals measured with VSD imaging reflect a mixture of spiking and subthreshold synaptic activity (9). To further examine the synaptic change underlying the priming effect of the real motion, we performed whole-cell recordings from V1 neurons in anesthetized mice, whose receptive fields (RFs) fell along one of the motion paths (Fig. 5 *A* and *B*). We then used the apparent and real motion stimuli similar to those used in the VSD imaging experiments. As expected, we found that the membrane potential responses evoked by a real motion across the RF ("on the path," Fig. 5*C*, red trace) were stronger than that in the alternate path ("off the path," blue trace). The difference between the responses showed two clear peaks, corresponding to the two sweeps of the real motion (Fig. 5 *D* and *E*). Importantly, although the subsequent apparent motion stimuli are identical in the two types of trials, the on-the-path response was significantly stronger than the off-the-path response for two sets of apparent motion stimuli. Moreover, we found no significant difference in the responses to the apparent motion stimuli before the real motion stimulation, indicating the observed difference was induced by the real motion stimulation. Thus, the real motion stimuli across the RF facilitated the synaptic responses to subsequent apparent motion stimuli for a period of ∼1 s, consistent with the result of the VSD imaging experiments.

Discussion

Multiple forms of bistable perception have been demonstrated at the psychophysical level, among which binocular rivalry (10) has been studied most extensively (11). A long-standing debate centered on the brain area at which the neural representation for the dominant percept is established. Whereas human fMRI studies suggest that the early visual circuits—lateral geniculate nucleus (LGN) (12, 13) and V1 (14–16)—play important roles in the competition, electrophysiological recordings in monkey V1 showed that most of these early neurons reflect the stimulus property rather than perception of the animal (17, 18). Several lines of evidence now suggest that binocular rivalry involves neural competition at multiple brain circuits (11, 19).

Apparent motion quartet provides another striking example of bistable perception. Because the perceptual competition occurs between spatially separated motion paths, V1 provides a suitable candidate circuit, given its precise retinotopic map. Our study has shown that a brief exposure to a real motion caused a transient facilitation of the cortical responses representing the motion path during subsequent presentation of apparent motion stimuli. However, whereas the priming effect of the real motion is long lasting at the perceptual level in human psychophysics experiments (Fig. S2), the effect observed in mouse V1 was much more transient. This discrepancy may be attributed to two different causes. First, there may exist some species difference in the persistence of the priming effect—short in mouse and long in human—and what we observed in mouse V1 could reflect the neural correlate of perception. Second, the transient signal in V1 found in mice only provides a biasing input to higher visual areas, where neural correlate of more persistent perception exists. We favor the second possibility, which is consistent with the view that V1 serves as a "highly adapted cortical lens" through which the higher brain areas perceive the visual information (20). Because bistable perception involves the competition between two equally plausible interpretations of the stimuli, a small facilitation of one neural representation may be sufficient to tip the balance and bias the perceptual outcome. Consistent with this notion, fMRI studies have suggested that the motion processing area MT (middle temporal area) plays an important role in the perception of bistable apparent motion (21, 22). Another potential approach in determining the role of V1 in the perception of bistable motion is to search for the existence of cortical correlates of spontaneous

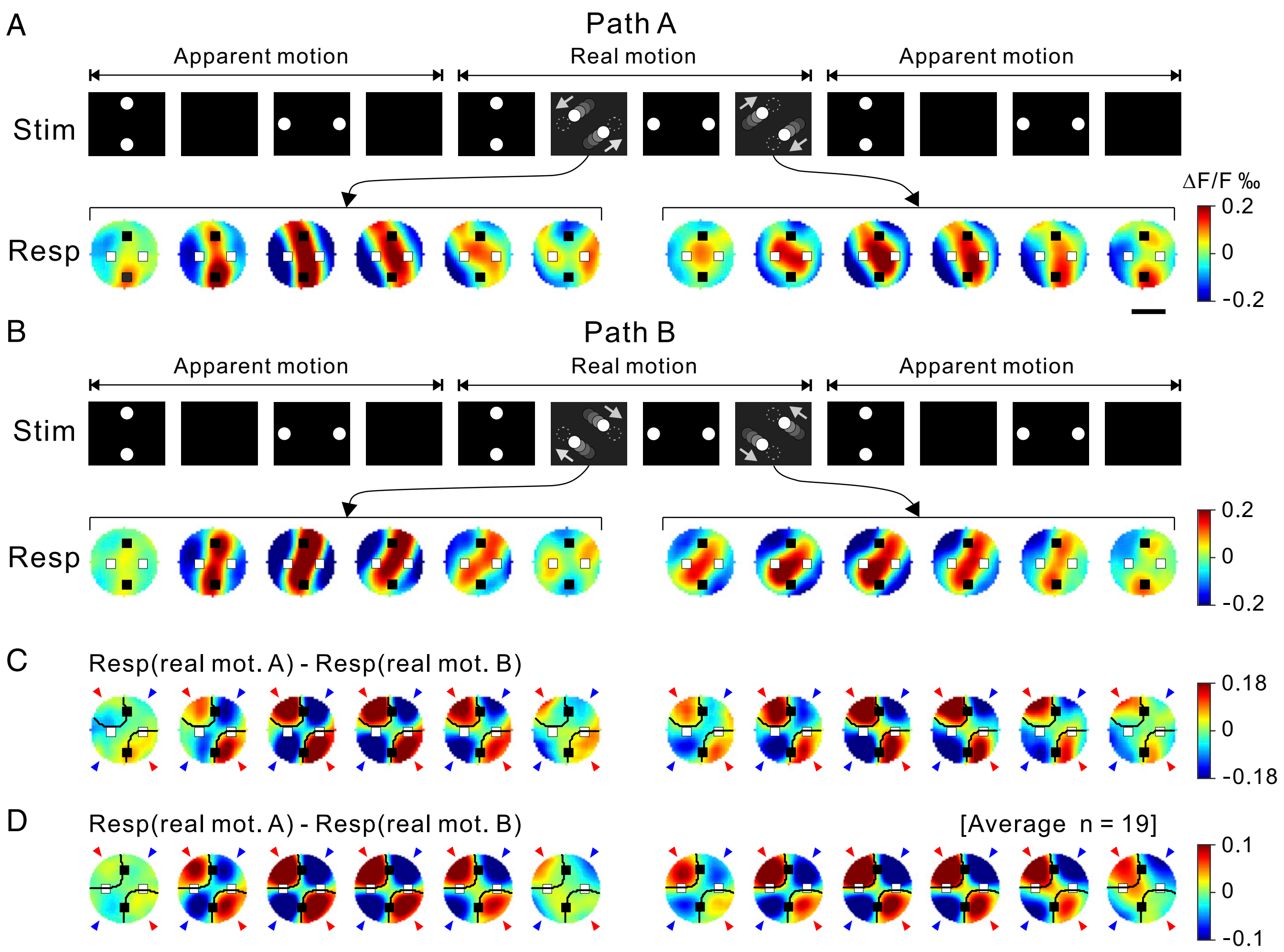

Fig. 2. VSD imaging of V1 responses to the real motion stimuli. (*A* and *B*, *Upper*) Stimulus sequence consisting of apparent motion quartet before (four cycles, only one shown) and after (six cycles, one shown) the real motion stimuli (one cycle) along path A and path B, respectively. (*Lower*) Example of VSD signals in response to the real motion stimulation along path A and path B, respectively. Each colorgram represents average signal over 30 ms (total time of one sweep of real motion: 180 ms), color coded with scale (*Right*). Black and white squares represent the region of maximal VSD signals evoked by the four flash dots illustrated in Fig. 1. (Scale bar, 500 μm.) (*C*) Difference of VSD responses ("Δ response") to the real motion along path A and path B for the example recording shown in *A* and *B*. Red and blue arrowheads mark the cortical regions representing path A and path B, respectively. Black contour lines depict cortical regions with strong positive Δ responses. (*D*) Average Δ response from all of the experiments (on 19 mice). Before averaging, the spatial patterns of cortical responses measured in each mouse were transformed (see text).

switching in the perception of bistable motion, a phenomenon well known in human psychophysics (Fig. S2). This would involve the detection of spontaneous switching of cortical activities representing the two apparent motion paths in V1. Unfortunately, this is at present not feasible using VSD imaging because averaging across multiple trials was required in our experiments due to the large variability of VSD signals.

A potential cellular basis for the perception of apparent motion is that neurons representing the regions along the illusory motion path are activated even though no physical stimuli are presented at these locations. Human fMRI experiments have indeed revealed BOLD signals in patches of V1 representing the illusory motion path (6), and VSD imaging experiments in anesthetized cats showed subthreshold cortical activity that could contribute to the perception of apparent motion in the line–motion illusion (9). Our study suggests that such subthreshold activity in the mouse V1 can be potentiated by a real motion stimulus, which may contribute to the bias in the perception of motion quartet. Mechanistically, this effect may be related to our recent finding that after repeated motion stimulus along a given path, a brief flash at the starting point of the motion path can evoke sequential firing among cortical neurons similar to that evoked by a real motion (23). Whereas potentiation of the spiking activity observed in the latter study requires multiple repeats of the real motion stimuli, we found in the current study that potentiation of the subthreshold activity could be induced by a single cycle of real motion.

With whole-cell recordings we could not determine whether the subthreshold synaptic inputs originate from local intracortical connections or long-range feedback connections from higher cortical areas. However, because our observations were from anesthetized animals, these responses were unlikely to reflect high-level cognitive feedback. Instead, it may reflect short-term plasticity of intracortical synaptic transmission (24) or intrinsic excitability of V1 neurons (25) that represent the motion path. At the perceptual level, multiple forms of priming have been demonstrated, in which recent exposure to a sensory stimulus facilitates its perception in later encounters (26). The short-term facilitation of the subthreshold activity in V1 shown here may reflect a basic mechanism that also contributes to other forms of perceptual priming.

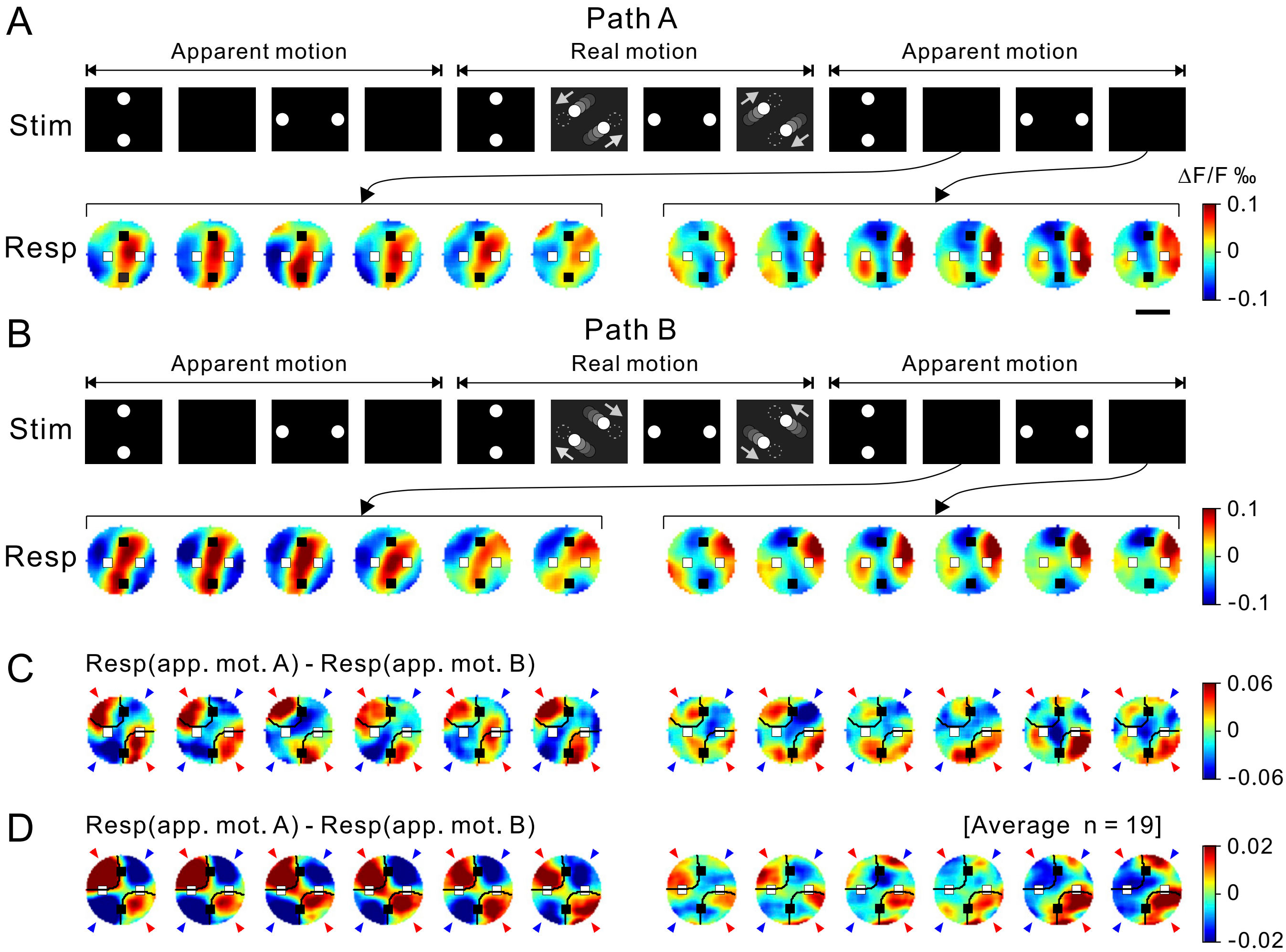

Fig. 3. VSD imaging of V1 responses to the apparent motion stimuli following the real motion. (*A* and *B*, *Upper*) stimulus sequence as in Fig. 2. (*Lower*) Example of VSD signals in response to the apparent motion stimuli immediately after the real motion along path A and path B, respectively. (Scale bar, 500 μm.) (*C*) Difference of VSD responses ("Δ response") to the apparent motion stimuli for the example recording shown in *A* and *B*. Red and blue arrowheads mark the cortical regions representing path A and path B, respectively. Black contour lines are the same as in Fig. 2*C*, representing cortical regions with strong positive Δ response to the real motion stimulation. (*D*) Average Δ response to apparent motion stimuli from all of the experiments (n = 19 mice).

Materials and Methods

Surgical Procedures and Preparation. The animal use protocol was approved by the Animal Use Committee of the Institute of Neuroscience, Shanghai Institutes for Biological Sciences, Chinese Academy of Sciences. Experiments were performed on adult C57BL/6J mice (50–90 d, 21–25 g). For head plate implant, mice were anesthetized with isoflurane (4% vol/vol initially, maintained at 1.5%) and placed on a stereotaxic frame (RWD Life Science; 68010). Body temperature was maintained at 37 °C with a regulated heating pad. The skin overlying the cortex was removed and the skull gently cleaned. For EEG recording, two screws were fixed to the skull in left and right hemispheres separately. The metal head plate was first glued to the skull by tissue adhesive (3M; Vetbond), with a 5.5 × 7 mm^2 hole above the primary visual cortex. Then the plate and screws were affixed to the skull via dental cement. The mice were allowed 2–4 d of recovery before the experiments.

Before the VSD imaging experiments, the implanted animals were anesthetized with isoflurane. A 4 × 4 mm^2 craniotomy was performed within the hole of the head plate. Voltage-sensitive dye RH1691 was dissolved in 1 mg/mL in a solution containing the following (in millimoles): 145 NaCl, 4 KCl, and 3 $CaCl_2$. The dye solution was applied topically to the exposed cortex within the head plate hole or within a chamber attached to the top of the head plate (via dental cement). The hole or the chamber was then capped or covered with a piece of plastic film. The mice were placed in the home cage for 4 h to allow recovery from anesthesia and staining of the cortex.

For whole-cell recording experiments, the mice were anesthetized with urethane (intraperitoneally, 2–2.7 g/kg). The body temperature was maintained at 37 °C with a regulated heating pad. A 2 × 1 mm^2 craniotomy and durotomy were performed over the visual cortex. The results were obtained from a total of 35 mice, for VSD imaging (19 mice) and whole-cell recording (16 mice).

Voltage-Sensitive Dye Imaging in Awake Mouse. The VSD imaging experiments were performed in awake head-fixed mice on a spherical treadmill (27), which consists of a Styrofoam ball (8-inch diameter) that can rotate freely about a fixed metal rod. The running speed of the mouse was recorded by an optical computer mouse placed near the ball. An infrared camera was used to observe whisking and grooming. With the help of an infrared light source (940 nm), the pupil position was monitored with another infrared camera. After the recording session the mouse was euthanized by the approved procedure.

Before imaging, the unbound dye was washed away, and the cortex was covered with 4% (wt/vol) agarose and a glass coverslip to decrease the movement of the cortex. Excitation light from a custom-made autostabilized light-emitting diode (LED) light source (630 nm/1 W; Cree) was filtered by a 632 ± 11 nm interference filter and reflected down onto the cortex by a 650-nm dichroic mirror. Fluorescence signals from the stained cortex were filtered with a 665-nm long-pass filter and collected by a high-speed MiCAM Ultima camera (BrainVision) with a 3.2 × 3.2 mm^2 field of view (100 × 100 pixels). Images were acquired with MiCAM Ultima software (BrainVision) at 5 ms per frame and analyzed in Matlab (MathWorks) using custom-written software. Recordings were performed when mice were quiet and the eye movement did not occur.

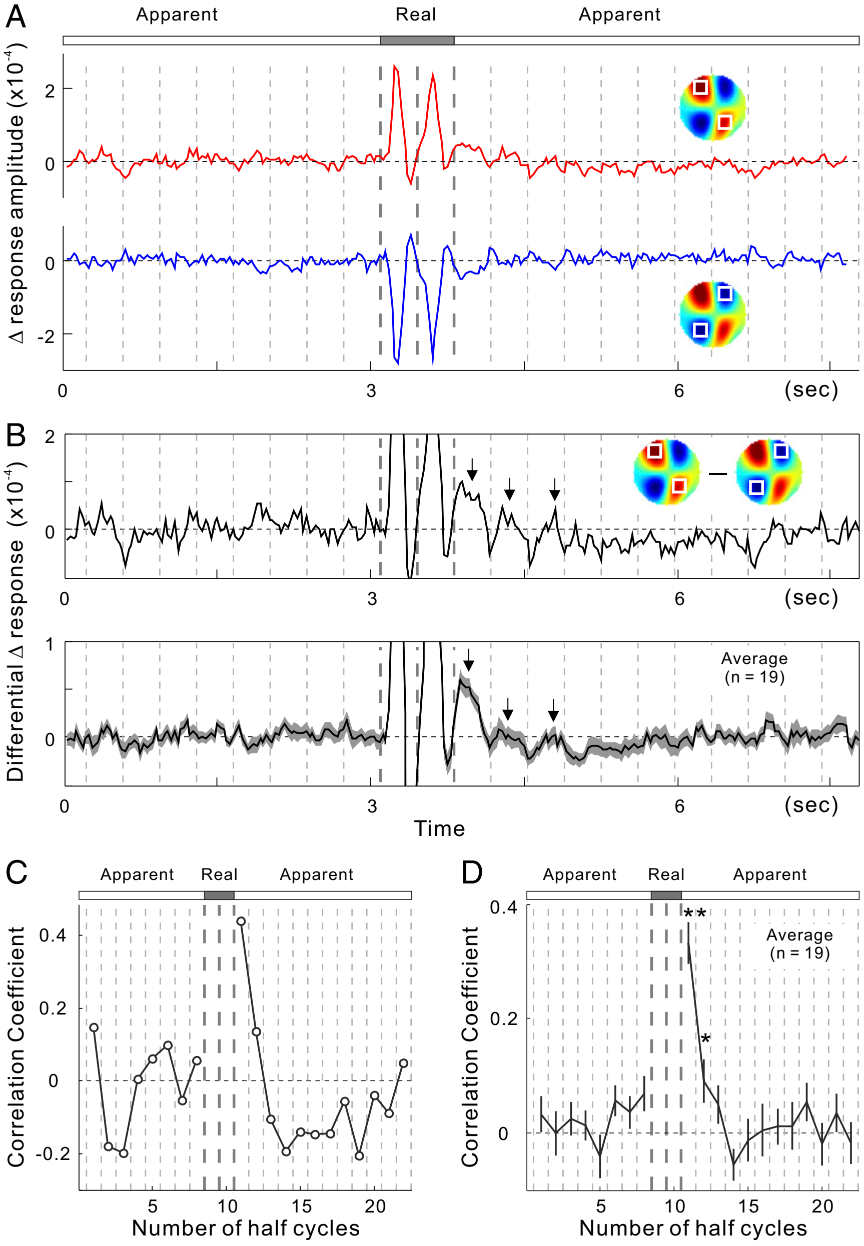

Fig. 4. Quantification of the effect of a real motion on cortical responses to apparent motion stimuli. (*A*) Amplitude of Δ response in the cortical regions representing path A (red) and path B (blue) from the example experiment shown in Figs. 2 and 3. Dashed gray lines mark the starting time of each apparent (light gray) or real (dark gray) motion. White square (*Inset*) indicate the region in which the amplitude was measured. (*B*) Difference in the amplitude of Δ response between the cortical regions representing path A and path B. (*Upper*) For the example shown in *A*. (*Lower*) Average across all experiments ($n = 19$). Shaded area indicates ± SEM. Arrows mark the oscillations at the temporal frequency of real motion. (*C* and *D*) Correlation coefficients between Δ response for a single sweep of real motion (template) and each set of apparent motion, for the example shown in *A* and *B* and the average of all experiments ($n = 19$; $^{**}P = 3 \times 10^{-8}$, $^{*}P = 0.025$).

Whole-Cell Recording in Anesthetized Mice. Whole-cell recordings were made with an Axopatch 700A amplifier (Axon Instruments) in the current clamp mode. Patch pipettes (7–8.5 MΩ) were filled with internal solution containing (in millimoles) 120 K-gluconate, 10 KCl, 5 NaCl, 1 MgCl2, 10 Hepes, 0.2 EGTA, 2 ATP-Mg, 0.5 GTP-Na, 10 phosphocreatine di(Tris), and some beads (5 μm; Bangs Laboratories). Data were sampled at 10 kHz,digitized by Digidata 1332A (Axon Instruments), and analyzed with custom software in Matlab.

For each recorded cell, the RF was measured by sparse noise and reverse correlation (28). The quartet dot stimuli were positioned such that the RF of the recorded cell fell along one of the motion paths. Visual stimuli were similar to those used in VSD imaging experiments. For each cell, the responses were averaged from 10 to 40 trials.

Visual Stimulation. Visual stimuli were generated with a Windows-based personal computer equipped with a NVIDIA Quandro FX 1700 graphics board and presented via a 17-inch liquid crystal display (LCD) monitor (34 × 27 cm, 800 × 600 pixels, 75 Hz, maximum luminance 70 cd/m^2), which was placed at 12.5 cm from the contralateral eye.

To determine the retinotopic representation of the dot quartet, a bright circular dot (7° visual angle) was flashed briefly (100 ms, 70 cd/m^2) at each of the four positions (Fig. 1). To measure the effect of real motion on the responses to apparent motion stimuli, each trial (2,048 frames, 10.24 s) consisted of four cycles of apparent motion quartet, one cycle of real motion, followed by six more cycles of apparent motion. Each cycle includes a forward and a backward sweep (real motion) or jump (apparent motion). For apparent motion quartet, a pair of dots (7° visual angle, 70 cd/m^2) was flashed alternately at the ends of two diagonals of an invisible diamond (43° by 28° visual angle) (Fig. 2). The dots were presented at each position for 180 ms and off for 180 ms before appearing at the alternate positions. During the real motion period, each dot was presented at the fixed location for 180 ms and moved along the path for 180 ms (Fig. 2 *A* and *B*), with a velocity of 142°/s. The stimulus with path A or path B real motion was randomly presented, with equal total trial number for path A and path B. In each animal, a total of 40–160 trials were recorded, with an intertrial interval of 90–120 s. The data were grouped according to the stimulus (path A or B) and averaged within the group.

Data Analysis. For VSD imaging experiments, the trial was discarded if the running speed of mice exceeded 20 mm/s, as monitored by the optical computer mouse. For each trial, we calculated ΔF/F as $[F(x, y, t) - F(x, y, t_0)]/F(x, y, t_0)$, where $F(x, y, t)$ represents the fluorescence signal at location *x*, *y*

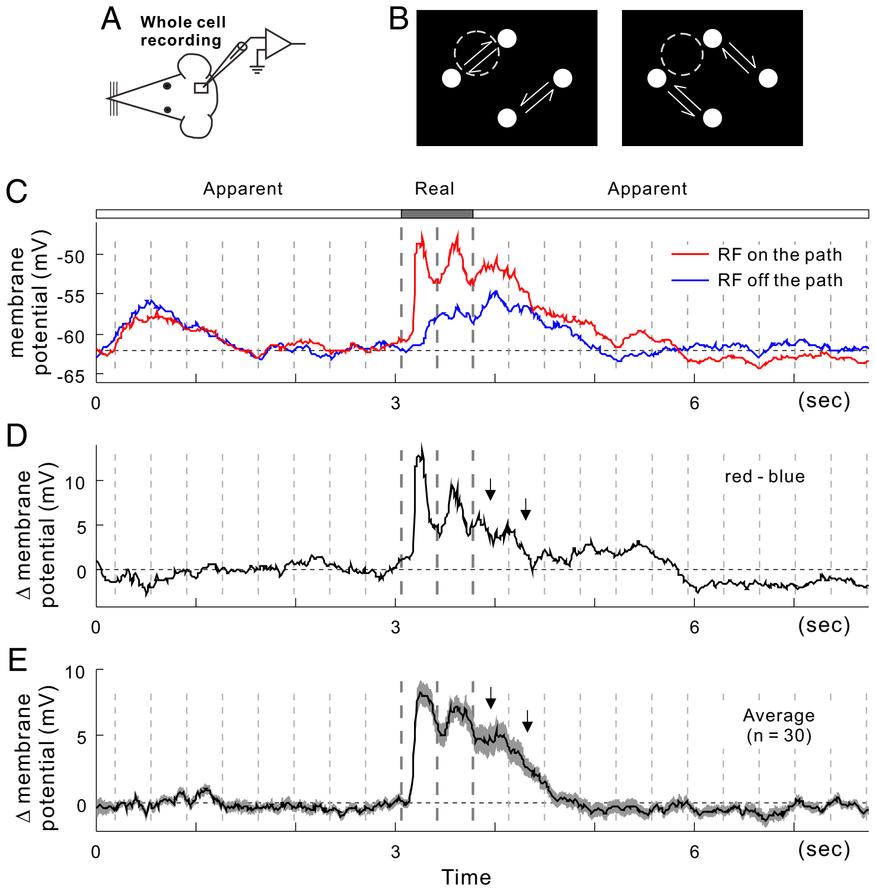

Fig. 5. Whole-cell recordings from V1 neurons in anesthetized mice. (*A*) Schematic diagram of whole-cell recording experiment. (*B*) Illustration of the RF of recorded neuron (dashed circle) relative to the quartet dot stimuli. (*C*) Example recording of membrane potential responses before, during, and after the real motion, in trials with the RF on the path (red) and off the path (blue) of real motion. Dashed gray lines mark the starting time of each apparent (light gray) or real (dark gray) motion. (*D*) Difference between membrane potential responses on the path (red) and off the path (blue) for the example shown in *C*. Arrows mark the differential depolarization following the real motion stimulation. (*E*) Average difference in membrane potential response across all experiments ($n = 30$ cells). Shaded area indicates ± SEM.

and time t, and t_0 represents the time of the first frame in each trial. We then applied a 2D spatial filter (boxcar, 96 × 96 μm) to the image in each frame. To correct the baseline shift in individual trials, we normalized the signal by subtraction of the average signal over the period without stimulation and the apparent motion period before real motion test. Spatial bandpass filter (300~800 μm) was applied to further remove the noise and fluctuation. To average the data across VSD imaging experiments, the responses from each mouse were rotated and stretched into an idealized cortical map in which the maximal responses to the four dots fell on a perfect diamond, using the Matlab function "imtransform."

ACKNOWLEDGMENTS. We thank Weifeng Xu, Xin Gao, and Chun-feng Shang for technical help. This work was supported by the National Basic Research Program of China (2011CBA00400).

1. Rees G, Kreiman G, Koch C (2002) Neural correlates of consciousness in humans. *Nat Rev Neurosci* 3(4):261–270.
2. Sterzer P, Kleinschmidt A, Rees G (2009) The neural bases of multistable perception. *Trends Cogn Sci* 13(7):310–318.
3. Ramachandran VS, Anstis SM (1985) Perceptual organization in multistable apparent motion. *Perception* 14(2):135–143.
4. Carter O, Konkle T, Wang Q, Hayward V, Moore C (2008) Tactile rivalry demonstrated with an ambiguous apparent-motion quartet. *Curr Biol* 18(14):1050–1054.
5. Yantis S, Nakama T (1998) Visual interactions in the path of apparent motion. *Nat Neurosci* 1(6):508–512.
6. Muckli L, Kohler A, Kriegeskorte N, Singer W (2005) Primary visual cortex activity along the apparent-motion trace reflects illusory perception. *PLoS Biol* 3(8):e265.
7. Anonymous (2009) Connecting the dots. *Nat Neurosci* 12(2):99.
8. Logothetis NK, Wandell BA (2004) Interpreting the BOLD signal. *Annu Rev Physiol* 66:735–769.
9. Jancke D, Chavane F, Naaman S, Grinvald A (2004) Imaging cortical correlates of illusion in early visual cortex. *Nature* 428(6981):423–426.
10. Wheatstone C (1962) On some remarkable and hitherto unobserved phenomena of binocular vision. *Optom Wkly* 53:2311–2315.
11. Tong F, Meng M, Blake R (2006) Neural bases of binocular rivalry. *Trends Cogn Sci* 10 (11):502–511.
12. Wunderlich K, Schneider KA, Kastner S (2005) Neural correlates of binocular rivalry in the human lateral geniculate nucleus. *Nat Neurosci* 8(11):1595–1602.
13. Haynes JD, Deichmann R, Rees G (2005) Eye-specific effects of binocular rivalry in the human lateral geniculate nucleus. *Nature* 438(7067):496–499.
14. Lee SH, Blake R, Heeger DJ (2005) Traveling waves of activity in primary visual cortex during binocular rivalry. *Nat Neurosci* 8(1):22–23.
15. Polonsky A, Blake R, Braun J, Heeger DJ (2000) Neuronal activity in human primary visual cortex correlates with perception during binocular rivalry. *Nat Neurosci* 3(11):1153–1159.
16. Tong F, Engel SA (2001) Interocular rivalry revealed in the human cortical blind-spot representation. *Nature* 411(6834):195–199.
17. Leopold DA, Logothetis NK (1996) Activity changes in early visual cortex reflect monkeys' percepts during binocular rivalry. *Nature* 379(6565):549–553.
18. Sheinberg DL, Logothetis NK (1997) The role of temporal cortical areas in perceptual organization. *Proc Natl Acad Sci USA* 94(7):3408–3413.
19. Wilson HR (2003) Computational evidence for a rivalry hierarchy in vision. *Proc Natl Acad Sci USA* 100(24):14499–14503.
20. Leopold DA (2012) Primary visual cortex: Awareness and blindsight. *Annu Rev Neurosci* 35:91–109.
21. Genç E, Bergmann J, Singer W, Kohler A (2011) Interhemispheric connections shape subjective experience of bistable motion. *Curr Biol* 21(17):1494–1499.
22. Sterzer P, Haynes JD, Rees G (2006) Primary visual cortex activation on the path of apparent motion is mediated by feedback from hMT+/V5. *Neuroimage* 32(3):1308–1316.
23. Xu S, Jiang W, Poo MM, Dan Y (2012) Activity recall in a visual cortical ensemble. *Nat Neurosci* 15(3):449–455.
24. Zucker RS, Regehr WG (2002) Short-term synaptic plasticity. *Annu Rev Physiol* 64: 355–405.
25. Zhang W, Linden DJ (2003) The other side of the engram: Experience-driven changes in neuronal intrinsic excitability. *Nat Rev Neurosci* 4(11):885–900.
26. Tulving E, Schacter DL (1990) Priming and human memory systems. *Science* 247(4940): 301–306.
27. Dombeck DA, Khabbaz AN, Collman F, Adelman TL, Tank DW (2007) Imaging large-scale neural activity with cellular resolution in awake, mobile mice. *Neuron* 56(1):43–57.
28. Jones JP, Palmer LA (1987) The two-dimensional spatial structure of simple receptive fields in cat striate cortex. *J Neurophysiol* 58(6):1187–1211.